Proceedings of the 5th International Conference on Information Technology and Application in Biomedicine, in conjunction with
The 2nd International Symposium & Summer School on Biomedical and Health Engineering
Shenzhen, China, May 30-31, 2008

Regularization in Super-resolution Reconstruction of Biomedical Images using Gradient Vector Field

Xin Zhang, and Edmund Y. Lam

***Abstract*— The paper presents a method for regularization parameter in super-resolution reconstruction of biomedical images using the gradient vector field of a preliminary high resolution image. This works well in suppressing artifacts and excessive smoothing compared with Tikhonov regularization. Experiments of synthetic and real MRI images are presented to verify the performance of reconstruction.**

I. INTRODUCTION

High resolution (HR) images are frequently required in biomedical applications, because HR images provides the accurate spatial and intensity information to investigators. The requirements often imply upgrading in imaging facilities. But the modification brings improvements are limited by the cost and subsequent changes in existent parameters. So super-resolution reconstruction is used to reconstruct an HR image based on obtainable low resolution (LR) images. In recent years, it has been applied to several imaging modalities, including MRI [1], [2], [3], optical coherence tomography (OCT) [4], [5], *in vivo* ultrasound imaging [6], and PET [7]. Relatively LR images are more easily obtained. They are insufficient to provide an accurate visualization of the interest, and only one LR image is also hardly possible to reconstruct an HR image. Fortunately, in certain medical imaging modalities, LR images are often provided as a set. Each of them can bring different desirable information of a focused object. The technology lays a foundation for super-resolution reconstruction, which collects together the different information behind LR images and reconstruct an HR image.

The reconstruction is typically an ill-posed problem, which means a small perturbation in the input would produce a huge unexpected disturbance in the output. A variety of regularization techniques have been proposed, such as half-quadratic regularization (HQR) [8], [9], [10], [11], [12] , directional regularization [13], [14], [15] and adaptive regularization [16], [17], [18]. Nevertheless, Tikhonov regularization is still one of the most commonly used methods to solve the ill-posed problem because of easy implementation and speed. The regularization is used to form a constraint and transforms the problem into a minimization. Though it has such advantages in implementation, the resulting image is often not able to preserve edges and possibly affected by a global smoothness and even ringing artifacts. An explanation of the phenomenon is attributed to the regularization parameter, which manages the degree to which the regularization is performed on the problem. Choosing appropriate regularization parameters have been discussed in [20], [21], [22]. We propose the adaptive choice of the regularization parameter to handle the balance. The assignment is useful to execute regularization appropriately.

Xin Zhang and Edmund Y. Lam are with the Department of Electrical and Electronic Engineering, The University of Hong Kong, Pokfulam Road, Hong Kong. Corresponding author email: elam@eee.hku.hk.

The paper is structured as follows. In Section 2, we describe the model we use in the reconstruction and propose the adaptive choice of regularization parameters. Tikhonov regularization is introduced pertaining to the problem. Section 3 shows the results of experiments using a synthetic image and MRI brain image. Section 4 concludes this paper.

II. OBSERVATION MODEL AND REGULARIZATION

In medical image processing applications, a true image f can be related to degraded data y through a linear model of the form

$$y = Hf + n, \tag{1}$$

where H is the system matrix and n denotes noise.

Let us consider a special case of super-resolution reconstruction in which four low resolution (LR) images of size $N \times N$ are used. The target HR image is of size $2N \times 2N$. We can use a raster scan of the matrices so that the vectors y, f, and n are all of size $4N^2$, while H is a matrix of size $4N^2 \times 4N^2$. The problem is to determine f from the observation y and knowledge of H and is a typical ill-posed inverse problem.

It is necessary to rely on a regularization to stabilize the inversion of ill-posed problem. Through the regularization, the problem (1) is replaced by the one of seeking an estimate f to minimize the Lagrangian:

$$\min_f \left[\|y - Hf\|_2^2 + \alpha \|Cf\|_2^2 \right] , \tag{2}$$

where the operator C is generally a high-pass filter, and $\|\cdot\|$ represents L_2 norm. The first term measures the fidelity of the solution to the data while the second term manages the smoothness of the solution. α denotes the Lagrange multiplier, commonly referred to as the regularization factor. C is often chosen as the Laplacian operator to smooth the solution. So the minimizer of (2) expressed as normal equations is

$$H^T y = (H^T H - \alpha C^T C) f. \tag{3}$$

The regularization parameter α controls the degree of regularization on the reconstruction. To choose the parameter appropriately, we propose to determine it according to the local gradient of a preliminary HR image. We can form a

○	△	○	△	○	△	○	△
▽	⋆	▽	⋆	▽	⋆	▽	⋆
○	△	○	△	○	△	○	△
▽	⋆	▽	⋆	▽	⋆	▽	⋆
○	△	○	△	○	△	○	△
▽	⋆	▽	⋆	▽	⋆	▽	⋆
○	△	○	△	○	△	○	△
▽	⋆	▽	⋆	▽	⋆	▽	⋆

Fig. 1. The diagram of a preliminary HR image. ○ is an element in the first LR image, △ the second LR, ▽ the third LR image and ⋆ the fourth one.

preliminary HR image through reorganizing the pixel values of the four LR images, shown in Fig. 1. ○, △, ▽ and ⋆ represent elements in the four LR images, respectively.

This is different from the one generally used in regularization methods. Most of them use a global parameter to regularize the whole image. Here the parameter is a vector and ith element weights the regularization on f_i, ith element in f. Its configuration is related to the magnitude of the gradient vector field of the preliminary HR image and estimated by the expression:

$$\alpha_i = \alpha_{\min}\big[1 - \exp(-k|\nabla f_i|)\big] + \alpha_{\max}\exp(-k|\nabla f_i|), \quad (4)$$

where $|\nabla f_i|$ stands for the magnitude of gradient vector at f_i, k controls the rate of exponential decrease, and $\alpha_{\min}$ and $\alpha_{\max}$ are the minimal and maximal values of the parameter. When a reconstructed image is over smoothed, the regularization parameter is chosen as the maximum $\alpha_{\max}$. When the image is too rough, the parameter corresponds the minimum $\alpha_{\min}$. Combining properties of medical images, we can evaluate an appropriate value for every element of the parameter through three factors, k, α_{min} and α_{max}. The design of α vector is also different from the existing methods such as the discrepancy principle, generalized cross-validation and the *L*-curve [23]. Local gradient information is utilized to determine where and to what degree of regularization should be imposed, which is advantageous at restoring local edges and suppressing noise according to local information.

To evaluate the reconstruction using regularization with a gradient vector field, we will compute the peak signal-to-reconstructed image (PSNR). Assume both an original HR image $f_0(i,j)$ and degrading process H are known. Perform the reconstruction on these images to get the final image $f(i,j)$. The mean squared error (MSE) of the reconstructed image is

$$MSE = \frac{\sum [f(i,j) - f_0(i,j)]^2}{4N^2}. \quad (5)$$

The summation is over all pixels. The root mean squared error (RMSE) will be the square root of MSE. PSNR is measured by using

$$PSNR_{dB} = 20\log_{10}\left(\frac{255}{RMSE}\right). \quad (6)$$

III. RESULTS

Two sets of experiments are employed to evaluate the performance of adaptive regularization in super-resolution reconstruction of medical images. Simulation experiment is applied on a representative image (Shepp-Logan phantom) of medical image processing. It is synthetic and of size 256 $\times$ 256, shown in Fig. 2(a). White Gaussian noise corrupts the image so that SNR of the HR image stays at 28.82 dB. The noisy image is shifted and downsampled to generate four LR (128 $\times$ 128) images. Take the four images as input to reconstruct an HR image. One of them is shown in Fig. 2(b). In Fig. 2, the lower left image is from the reconstruction of common Tikhonov regularization and the lower right one is obtained by our modified Tikhonov regularization.

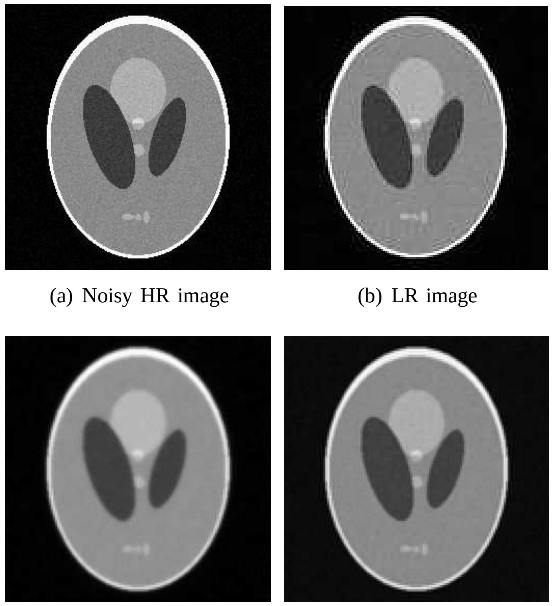

(a) Noisy HR image (b) LR image

(c) TR recons. image (d) MTR recons. image

Fig. 2. Involved images in the simulation. Shown are the HR image (a), one of LR images (b), reconstructed image (c) and (d) by Tikhonov regularization and the modified regularization, respectively.

Compared with the LR image, the reconstructed one is clear and presents accurately structure information of human brain. The smoothness of regularization reduces the noise in results. The effect is shown up in the reconstructed image. The comparison between reconstructed and original HR image makes the effect more visible.

The simulation is allowed us to measure PSNR. The original HR image is $f(i,j)$ and reconstructed one is $F(i,j)$ in 5. PSNR value is 31.16 dB and 33.16 dB in the reconstruction using Tikhonov regularization and our modified one. Typical PSNR values range from 20 to 40 dB. That demonstrates the whole reconstruction procedure is acceptable, it collects useful information of LR images into the final result and it doesn't incur noticeable noise at the same time. Moreover, modified regularization has a better performance than the common Tikhonov regularization.

Experiments are also performed on human brain MRI images. It aims to analyze the reconstruction on MRI images.

Both MSE and PSNR are measured to manifest the accuracy. The original HR image is 256 $\times$ 256.

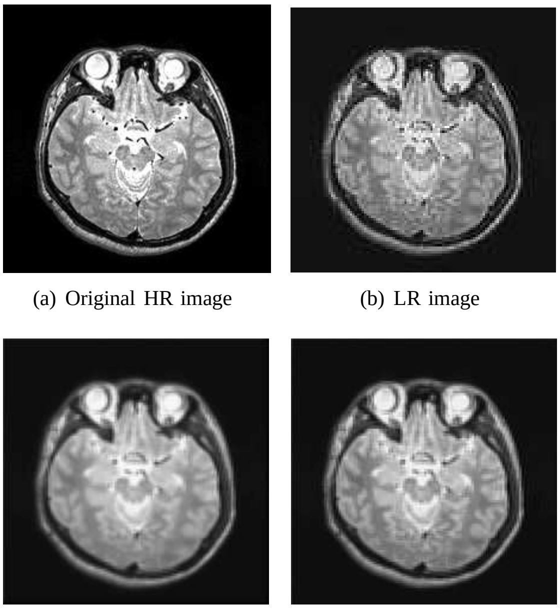

(a) Original HR image (b) LR image

(c) TR recons. image (d) MTR recons. image

Fig. 3. Images of MRI reconstruction experiments. Shown are the HR image (a), one of LR images (b), reconstructed image (c) and (d) by Tikhonov regularization and the modified regularization, respectively.

PSNR is 30.16 dB and 33.08 dB in the reconstruction of Tikhonov regularization and modified one. It verifies the modified Tikhonov regularization is advantageous over the common one in real medical images, thanks to the optimal choosing of regularization parameter.

IV. CONCLUSIONS

In this work, we investigate the implementation of adaptively choosing the parameters of Tikhonov regularization to perform super-resolution reconstruction in medical images and compare it with common Tikhonov regularization in reconstructions. Both experiments using synthetic medical image and real MRI images show our method assigns a more appropriate degree of regularization on the reconstruction and it is effective to produce a better image, which both preserves edges and removes noise. Adaptive parameter works well to improve Tikhonov regularization in super-resolution reconstruction of medical images.

ACKNOWLEDGMENT

This work was supported in part by the University Research Committee of the University of Hong Kong under Grant Number URC-10207440.

REFERENCES

[1] S. Peled and Y. Yeshurun, "Superresolution in MRI : Application to human white matter fiber tract visualization by diffusion tensor imaging," *Magn. Reson. Imaging*, vol. 45, no. 1, pp. 29–35, Jan. 2001.

[2] H. Greenspan, S. Peled, G. Oz, and N. Kiryati, "MRI inter-slice reconstruction using super-resolution," *Magn. Reson. Imaging*, vol. 20, no. 5, pp. 437–446, Feb. 2002.

[3] E. Carmi, S. Liu, N. Alon, A. Fiat, and D. Fiat, "Resolution enhancement in MRI," *Magn. Reson. Imaging*, vol. 24, no. 2, pp. 133–154, Feb. 2006.

[4] T. Blu, H. Bay, and M. Unser, "A new high-resolution processing method for the deconvolution of optical coherence tomography signals," in *IEEE International Symposium on Biomedical Imaging*, Jul. 2002, pp. 777–780.

[5] T. Blu, "Superresolution in optical coherence tomography," in *International Conference on Super-Resolution Imaging: Theory, Algorithms and Applications*, Aug. 2005, p. 4.

[6] G. T. Clement, J. Huttunen, and K. Hynynen, "Superresolution ultrasound imaging using back-projected reconstruction," *Journal of the Acoustical Society of America*, vol. 118, no. 6, pp. 3953–3960, Dec. 2005.

[7] J. Kennedy, O. Israel, A. Frenkel, R. Bar-Shalom, and H. Azhari, "Super-resolution in PET imaging," *IEEE Trans. Medical Imaging*, vol. 25, no. 2, pp. 137–147, Feb. 2006.

[8] P. Charbonnier, L. Blanc-Féraud, G. Aubert, and M. Barlaud, "Deterministic edge-preserving regularization in computed imaging," *IEEE Trans. Imag. Proc.*, vol. 6, no. 2, pp. 298–311, Feb. 1997.

[9] M. Nikolova and M. K. Ng, "Fast image reconstruction algorithms combining half-quadratic regularization and preconditioning," in *Proceedings of 2001 International Conference on Image Processing*, vol. 1, Oct. 2001, pp. 277–280.

[10] M. K. Ng, "Half-quadratic regularization, preconditioning and application," in *Proceedings of 2001 International Symposium on Intelligent Multimedia, Video and Speech Processing*, May 2001, pp. 32–35.

[11] ——, "Comparison of the main forms of half-quadratic regularization," in *Proceedings of 2002 International Conference on Image Processing*, vol. 1, Sep. 2002, pp. 349–352.

[12] R. Deriche, P. Kornprobst, M. Nikolova, and M. Ng, "Half-quadratic regularization for MRI image restoration," in *Proceedings of 2003 IEEE International Conference on Acoustics, Speech and Signal Processing*, vol. 6, Apr. 2003, pp. 585–588.

[13] S. Lee and C. Lee, "A new space-adaptive regularized constrained iterative image restoration algorithms and analysis of convergence condition," in *Proceedings of International Conference on Image Processing, 1996*, vol. 1, Sep. 1996, pp. 781–784.

[14] S. Lee, N. Moon, and C. Lee, "Recovery of blurred video signals using iterative image restoration combined with motion estimation," in *Proceedings of International Conference on Image Processing, 1997*, vol. 1, Oct. 1997, pp. 755–758.

[15] S. Lee, H. Cho, and J.-I. Park, "Directional regularisation for constrained iterative image restoration," *Electronics Letters*, vol. 39, no. 23, pp. 1642–1643, Nov. 2003.

[16] W. Vanzella, F. A. Pellegrino, and V. Torre, "Self-adaptive regularization," *IEEE Trans. Pattern Analysis and Machine Intelligence*, vol. 26, no. 6, pp. 804–809, Jun. 2004.

[17] D. Watzenig, B. Brandstätter, and G. Holler, "Adaptive regularization parameter adjustment for reconstruction problems," *IEEE Trans. Magn.*, vol. 40, no. 2, pp. 1116–1119, Mar. 2004.

[18] Y.-S. Choi, H.-C. Shin, and W.-J. Song, "Adaptive regularization matrix for affine projection algorithm," *IEEE Trans. Circuits Syst. II, Exp. Briefs*, vol. 54, no. 12, pp. 1087–1091, Dec. 2007.

[19] X. Zhang, E. Y. Lam, E. X. Wu, and K. K. Wong, "Application of Tikhonov regularization to super-resolution reconstruction of brain MRI image," in *Medical Imaging and Informatics*, Aug. 2007, pp. 46–51.

[20] N. P. Galatsanos and A. K. Katsaggelos, "Methods for choosing the regularization parameter and estimating the noise variance in image restoration and their relation," *IEEE Trans. Image Processing*, vol. 1, no. 3, pp. 322–336, Jul. 1992.

[21] S. Oraintara, W. C. Karl, D. A. Castanon, and T. Q. Nguyen, "A method for choosing the regularization parameter in generalized tikhonov regularized linear inverse problems," in *International Conference on Image Processing*, Oct. 2000, pp. 93–96.

[22] D. Strong, J.-F. Aujol, and T. Chan, "Scale recognition, regularization parameter selection, and meyer's g norm in total variation regularization," *SIAM Journal on Multiscale Modeling and Simulation*, vol. 5, no. 1, pp. 273–303, Jul. 2006.

[23] M. Kilmer and D. O'Leary, "Choosing regularization parameters in iterative methods for ill-posed problems," *SIAM J. Matrix Anal. Appl.*, vol. 22, no. 4, pp. 1204–1221, Apr. 2001.